International Journal of Microwave and Wireless Technologies

cambridge.org/mrf

A dual notched band UWB-BPF based on microstrip-to-short circuited CPW transition

Abu Nasar Ghazali[1], Mohd Sazid[2] and Srikanta Pal[3]

[1]School of Electronics, Kalinga Institute of Industrial Technology, Bhubaneswar, 751024, India; [2]Department of Electronics and Communication Engineering, Noida Institute of Engineering and Technology, Greater Noida, 201306, India and [3]Department of Electronics and Communication Engineering, Birla Institute of Technology, Mesra, Ranchi, 835215, India

Research Paper

Cite this article: Ghazali AN, Sazid M, Pal S (2018). A dual notched band UWB-BPF based on microstrip-to-short circuited CPW transition. *International Journal of Microwave and Wireless Technologies* **10**, 794–800. https://doi.org/10.1017/S1759078718000594

Received: 1 February 2018
Revised: 7 March 2018
Accepted: 7 March 2018
First published online: 21 May 2018

Key words:
Filters; microstrip bandpass filter; passive components and circuits

Author for correspondence:
Abu Nasar Ghazali, E-mail: anghazali@gmail.com

Abstract

This paper proposes a dual notched band ultra-wideband (UWB) bandpass filter (BPF) based on hybrid transition of microstrip and coplanar waveguide (CPW). The CPW in ground plane houses a stepped impedance resonator shorted at ends, and is designed to place its resonant modes within the UWB passband. The microstrips on the top plane are placed some distance apart in a back-to-back manner. The transition of microstrip on top and shorted CPW in the ground is coupled through the dielectric in a broadside manner. The optimized design of the transition develops the basic UWB spectrum with good return/insertion loss and extended stopband. Later, defected ground structure, embedded in CPW, and split ring resonators, coupled to feeding lines are utilized to develop dual sharp passband notches. The simulated data are verified against the experimentally developed prototype. The proposed dual notched UWB-BPF structure measures only 14.6×7.3 mm^2, thereby justifying its compactness.

Introduction

The ultra-wideband (UWB) communication technology is a blessing for the short-range communication systems due to its inherent high data rate capacity (≈1 Gb/s for <10 m) and non-interfering characteristics (low output power, −41.3 dBm/MHz) [1]. However, because of its ultra-wide bandwidth, it is prone to interference from other RF sources such as WLAN, C, X, band, etc., pocketed within the UWB spectrum, and might affect its performance considerably. To overcome these drawback researchers conceptualized and conceived UWB filters possessing integrated bandstop characteristics. These filters possess single or multiple bandstop characteristics depending upon the environment. Here we concentrate our design on UWB-bandpass filters (BPF) with dual notched band characteristics and the UWB literature is replete with such filters [2–12].

Slots etched in microstrips on the top plane develop dual notches in [2, 3], whereas structures coupled to the microstrips on a top plane in the form of electromagnetic bandgap structure (EBG), simplified composite right/left-handed resonator, E-shaped resonator, and stepped impedance resonator (SIR) develop multiple notches in [4–8], respectively. The structures proposed in [9, 10] develop dual notches based on wave cancellation method, whereas the use of defected ground structures (DGSs) inculcate dual passband notches in [11–13]. UWB filters with more than two notches have been reported in [14, 15]. However, most of the structures reported are quite large in size.

Here we propose a compact UWB-BPF with dual passband notches. The basic topology of our UWB filter is based on broadside coupled technology of microstrip-to-CPW, conceptualized in [16]. The basic structure of our proposed UWB filter consists of microstrips on a top plane arranged in a back-to-back manner, which are coupled with a short-circuited SIR-based CPW in the ground in broadside fashion. Later, multiple split ring resonators (SRRs) coupled to input/output (I/O) lines and spiral-shaped DGS (SDGS) etched in CPW are utilized to generate dual passband notches. Commercial full-wave EM software IE3D was used to design and optimize the proposed dual notched band BPF on a 0.635 mm-thick substrate, RT/Duriod 6010 with $\varepsilon_r = 10.8$ and loss tangent 0.0023. Later, the experimental structure is fabricated and tested for verification of the experimental data.

Proposed UWB filter

Basic UWB-BPF

The architecture of the proposed UWB-BPF is depicted in Fig. 1, from which we observe that the ground plane is made up of a short-circuited SIR-based CPW, whereas the top plane has two microstrip lines arranged at some distance in a back-to-back manner. This hybrid transition is capacitively linked through the dielectric to realize a broadside coupled UWB-BPF.

CAMBRIDGE UNIVERSITY PRESS

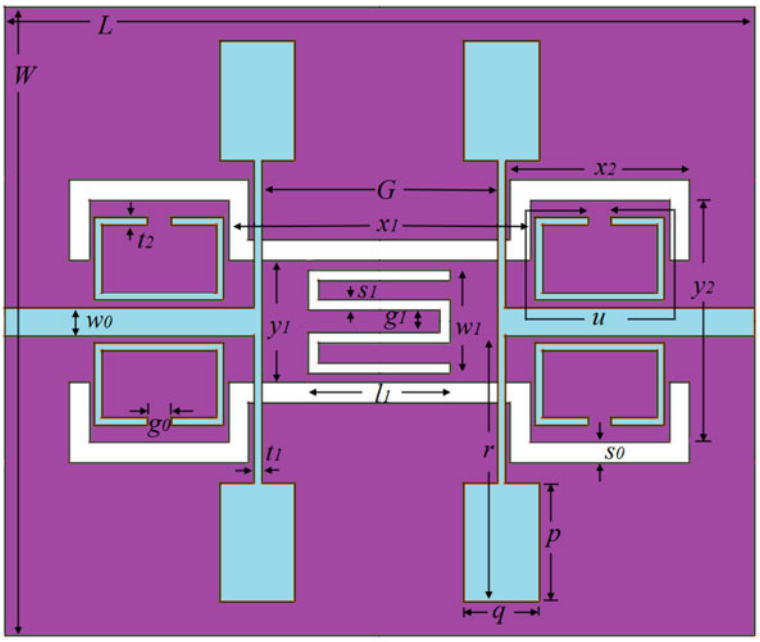

Fig. 1. Geometry of the proposed dual notched band UWB filter. Blue and purple shades represent conductors on top and ground planes, respectively, whereas white shade on ground plane depicts slots. All dimensions are marked in mm.

Initially, we develop the basic UWB-BPF to which SRRs and spirals are later added to develop multiple passband notches. We start our design analysis by considering the CPW-based SIR in the ground, depicted in Fig. 2(a). The analysis of CPW is pursued by neglecting the modified short-circuited edges because they have minimum effect on the response [17]. Several structures have been reported in the literature which makes use of the SIR as a multiple mode resonator to develop UWB-BPF response [18, 19]. Here, a similar analysis procedure has been adapted for the SIR. The arms of SIR are of electrical lengths $2\theta_1$, θ_2 and possess impedances Z_1, Z_2, respectively. The electrical lengths of the SIRs are related to each other via $\theta_1 \approx \theta_2$. The resonant modes of this SIR are functions of their impedance ratio, $k = Z_1/Z_2$, which is tuned so as to position its resonant modes quasi-equally within the passband. Figure 2(b) depicts the flexible positions of resonant modes for variable values of k. It can be observed from Fig. (2b), that for the chosen value of $k = 1.1$, the resonant modes at placed at 5.14 and 9.9 GHz, respectively. Also, the presence of a higher order harmonic at 13.8 GHz is observed. Figure 2(b) is the case of "weak coupling", and in order to develop the necessary UWB spectrum, this weak coupling needs to be alleviated to "tight coupling" through optimized modeling of the microstrip lines on the top. A tight coupling of the transition is obtained by matching the impedances of the transition (i.e., microstrip lines and central CPW section) via the relation, $Z_{0(\text{microstrip})} = 2Z_{0(\text{CPW1})}$ [16]. For the microstrip line with $t_1 = 0.15$ mm, $Z_{0(\text{microstrip})} = 83\ \Omega$, whereas for the central CPW section with $x_1 = 6.03$ mm, $y_1 = 2.46$ mm and $s_0 = 0.4$ mm, $Z_{0(\text{CPW1})} = 43.2\ \Omega$. According to [16], $Z_{0(\text{microstrip})} = 86.4\ \Omega$ should have been considered for perfect matching with $Z_{0(\text{CPW1})}$; however, a slightly deviant value of $Z_{0(\text{microstrip})} = 83\ \Omega$ is considered due to two reasons:

(i) For $Z_{0(\text{microstrip})} = 86.4\ \Omega$, the thickness of microstrip line would have been too thin leading to issues in fabrication, whereas
(ii) for $Z_{0(\text{microstrip})} = 83\ \Omega$ we get a better return/insertion loss.

Having achieved tight capacitive coupling of the transition, other parameters of the transition are tuned to improve the insertion

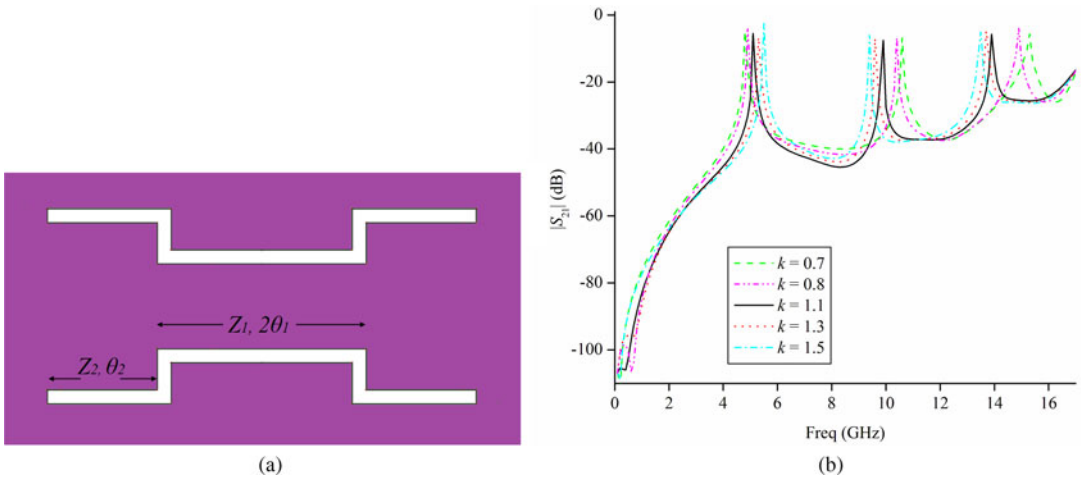

Fig. 2. (a) Approximate representation of the short-circuited SIR-based CPW. (b) Weak-coupling conditions for variable impedance conditions.

https://doi.org/10.1017/S1759078718000594 Published online by Cambridge University Press

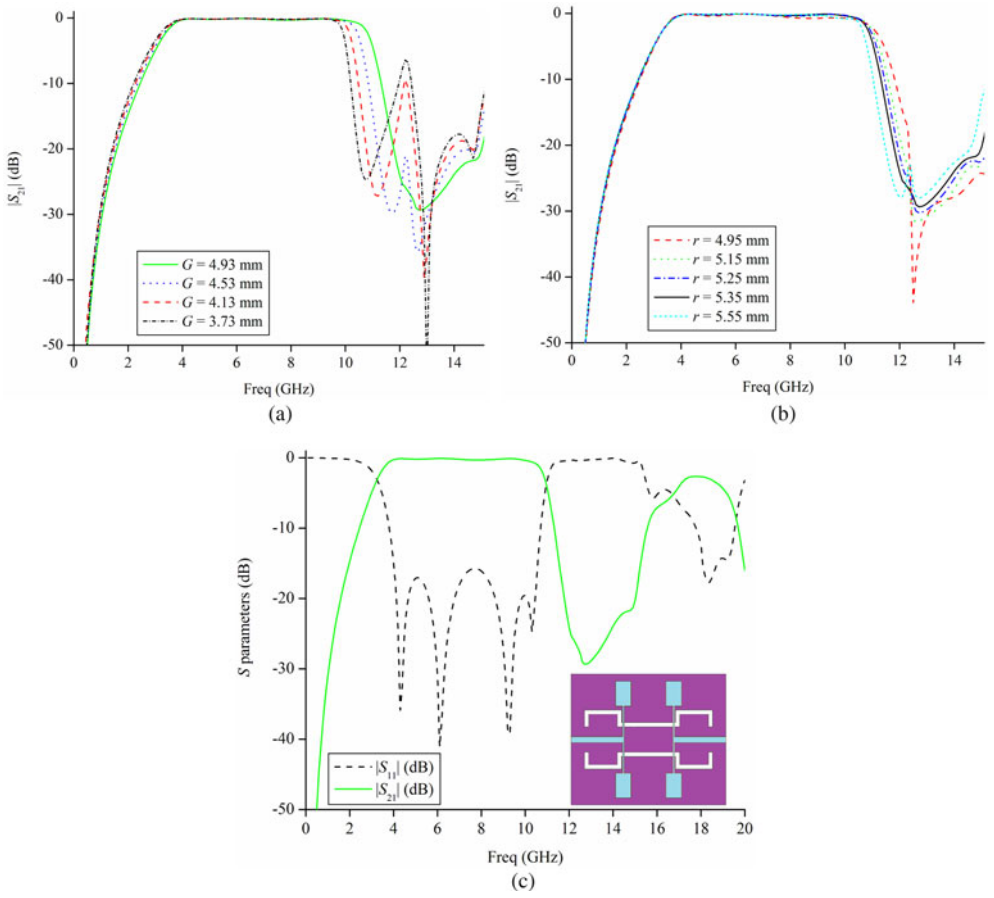

Fig. 3. (a) Tuning of transmission characteristics for variable spacing, *G*, between microstrip lines. (b) Tuning of transmission characteristics for variable length, *r*, of the microstrip lines. (c) Optimized simulated response of the basic broadside coupled UWB-BPF.

Table 1. Optimized dimensions of the basic UWB-BPF

Parameters	x_1	y_1	x_2	y_2	t_1	s_0	w_0	r	p	q	G	L	W
Dimensions (mm)	6.03	2.46	2.785	4.86	0.15	0.4	0.56	5.35	0.8	1.8	4.93	15	12.6

loss and adjust the position of higher cut-off frequency, respectively. Figures 3(a, b) demonstrate the tuning of UWB characteristics for a variable length of microstrip lines, *r*, and the distance, *G*, between them. The optimized response of the UWB-BPF is depicted in Fig. 3(c) and the final dimensions are mentioned in Table 1.

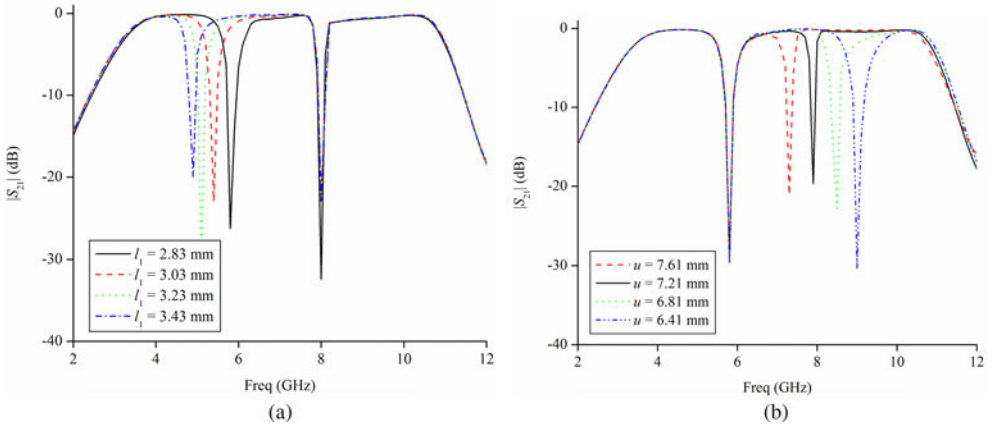

Fig. 4. Lower controllable notch for fixed dimensions of SRRs and variable length, l_1, of the SDGS. (b) Higher controllable notch for fixed dimensions of SDGS and variable length, *u*, of SRRs.

https://doi.org/10.1017/S1759078718000594 Published online by Cambridge University Press

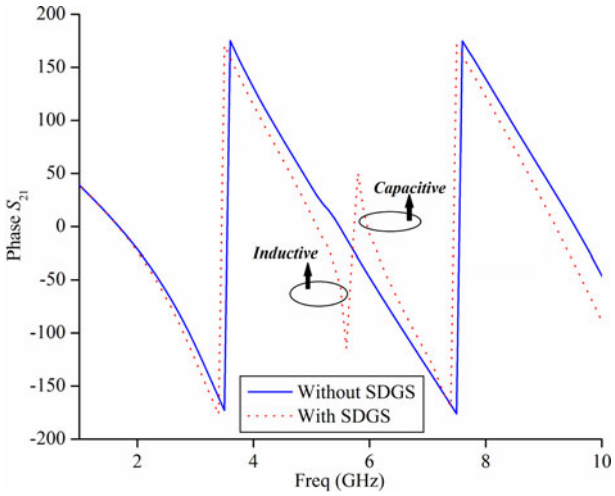

Fig. 5. Transmission phase characteristics of the UWB filter with and without SDGS units (all four SRRS units absent).

Band notched UWB filter

The ultra-wide spectrum of 3.1–10.6 GHz is home to several pockets of RF sources such as WLAN, C, X band, etc., and due to their high-energy output, they can act as a possible source of interference to the UWB communication systems. The UWB systems, on the other hand, due to their low output power, −41.3 dBm/MHz [1], seldom act as an interfering source. Hence, to overcome the interference problems UWB systems are often integrated with bandstop filter (BSF). However, appending a BSF with a BPF will bring about the increase in circuit size, which would be a disadvantage in this age of miniaturization. Keeping compactness as our prime motivation, we have developed a BSF-integrated BPF with the help of SDGS embedded in CPW and SRRs along the I/O feeding lines. We intend to place the dual notches at 5.8 GHz (WLAN) and 8 GHz (X band), due to SDGS and SRRs, respectively. The SDGS due to its long electrical length is able to place the notch deep within the passband and here it is designed to develop stopband at $f_{01} = 5.8$ GHz. The SRRs develop another notch at $f_{02} = 8$ GHz. Figures 4(a)

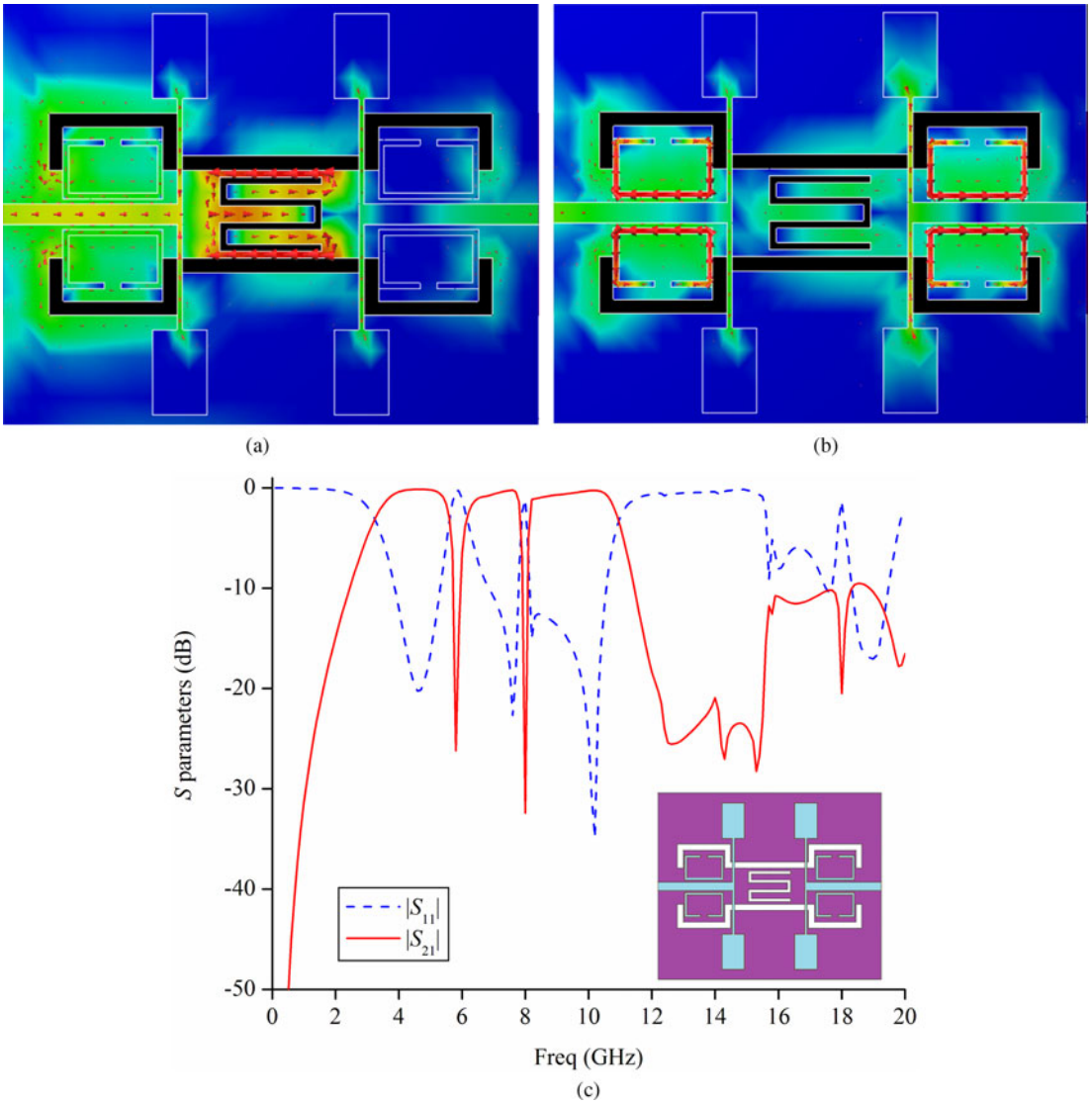

Fig. 6. (a) Current distribution in the UWB filter at 5.8 GHz. (b) Current distribution in the UWB filter at 8 GHz. (c) Optimized simulated response of the dual notched band UWB filter.

https://doi.org/10.1017/S1759078718000594 Published online by Cambridge University Press

Table 2. Optimized dimensions of the dual notched band UWB-BPF

Parameters	x_1	y_1	x_2	y_2	t_1	s_0	w_0	r	p	t_2
Dimensions (mm)	6.03	2.46	2.785	4.86	0.15	0.4	0.56	5.35	0.8	0.15
Parameters	q	G	L	W	u	g_0	l_1	w_1	s_1	g_1
Dimensions (mm)	1.8	4.93	15	12.6	7	0.46	2.83	2.06	0.2	0.46

and 4(b) depict the controllability of the notches for variable dimensions of the SDGS and SRRs. With the dimensions of SRRs fixed at u = mm, t_2 = mm, and g_0 = mm, Fig. 4(a) presents tunable lower notch positions for variable length, l_1, of the SDGS, whereas for variable length u of the SRRs and fixed length l_1 = mm of the SDGS, Fig. 4(b) depicts higher tunable notch. The lengths of SDGS and SRRs are about quarter of a guided wavelength at their respective notch frequencies.

Figure 5 depicts the comparative transmission phase characteristic (angle of S_{21}) of the UWB filter with and without notch at 5.8 GHz. The single notch is due to SDGS alone and for both cases all four SRRs are absent. The SDGS engraved filter characteristics depicts faster and slower variations in phase below and above the notch resonant frequency [11]. The reason is that when,

(1) $f < f_0$; $2\pi fL < 1/(2\pi fC)$, i.e. the capacitive reactance supersedes the inductive reactance and hence, current traverses the path of minimum resistance around the SDGS leading to increase of effective inductance, thus, faster phase variation is observed.
(2) For $f > f_0$; $2\pi fL > 1/(2\pi fC)$, i.e. the capacitive reactance is submissive to inductive reactance and hence, current traveling the path of minimum resistance moves across the SDGS causing the charge to accumulate at the slots which causes an increase in the effective capacitance, which in turn leads to slower phase variation.
(3) When $f = f_0$; $2\pi fL = 1/(2\pi fC)$, switching occurs at resonance.

Figure 6(a, b) depicts the current distribution in the proposed UWB filter at the dual notch frequencies from which it can be observed that for 5.8 GHz, the maximum current is concentrated around the SDGS, whereas for 8 GHz, the SRRs show increased current density concentration on them. These localized current densities around the SDGS and on the SRRs emphasize their pronounced effect on creating the respective notches compared with rest of the UWB parameters. The optimized frequency characteristics of the dual notched band UWB filter is plotted in Fig. 6(c). The optimized dimensions of the dual notched band UWB-BPF are mentioned in Table 2. The proposed structure is compared with other structures in Table 3.

It can be observed from Table 3, that the proposed structure meets the necessary UWB passband requirement with appreciable attenuation at the dual notch positions. The stopband is wide and deeper than 20 dB, thereby providing sufficient isolation. Also, the biggest feature of the proposed structure is its very compact size compared with the rest [2–13].

Experimental verification

In order to validate the data obtained through simulation, we developed an experimental prototype of the proposed structure and measured its frequency characteristics using Agilent Vector Network Analyzer N5230A. The measured data are compared with the simulated results in Fig. 7(a, b), from which deviation between the two is observed. This may be attributed to finite substrate size, unexpected fabrication tolerances, connector reflections, etc. Figure 7(a) depicts passband width from 3 to 10.9 GHz with dual notches centered at 5.96 and 8.15 GHz, respectively, and an extended stopband till 16 GHz possessing attenuation > 20 dB. The passband insertion/return loss is better

Table 3. Comparison of our proposed structure with other recently reported dual notched band UWB-BPF

Ref.	Passband (GHz)	Notch (GHz)/attenuation (dB)	Stopband (GHz)/attenuation	Size (mm × mm)
[2]	3.1–10.6	5.2, 5.8/>15	16/>15	>15 × 12
[3]	N.A	5.3, 5.775/>17	20/>15	>20 × 16
[4]	3.1–10.8	5.2, 5.8/>14	13/>18	32 × 20
[5]	3.1–10.9	5.8, 8.7/>14	16/>15	35 × 28
[6]	3.2–10.9	5.9, 8/>17	14/>25	24.7 × 12
[7]	2.97–11.18	5.8, 8.1/>20	20/>20	34.4 × 11.8
[8]	3.1–10.7	5.9, 8/>13	20/>13	27 × 17
[9]	2.8–11	4.3, 8/>18	14/>15	23.6 × 2.7
[10]	2.8–10.69	5.2, 8.04/>14	20/>15	23 × 15
[11]	2.5–12.2	5.15, 7.12/>18	18/>20	24 × 14.2
[12]	2.6–12	5.6, 8/>16	18/>16	22.2 × 14.2
[13]	2.8–11	5.3, 7.8/>20	30/>15	30 × 16
This work	3–10.9	5.96, 8.15/>15	16/>20	14.6 × 7.3

https://doi.org/10.1017/S1759078718000594 Published online by Cambridge University Press

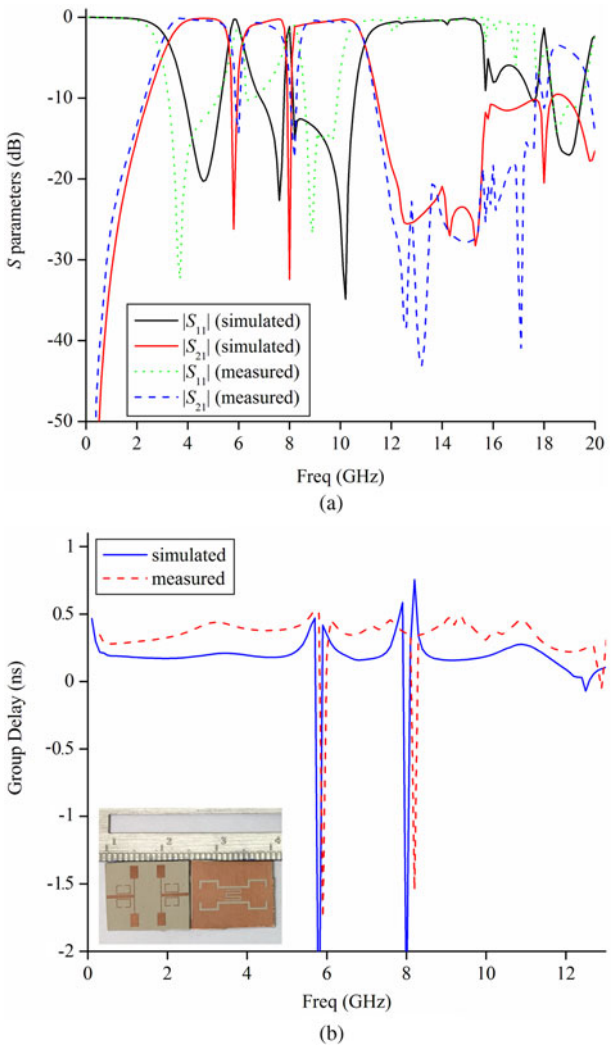

Fig. 7. (a) Comparative *S* parameters characteristics of the simulated and measured response. (b) Comparative measured and simulated group delay.

than 0.6 dB/15 dB between the lower cut-off frequency and the first notch (3–5.7 GHz), 0.86 dB/11 dB between the first and second notch (6.25–7.76 GHz), and 0.48 dB/17 dB after the second notch till the upper cut-off frequency (8.451–10.9 GHz). The measured group delay, plotted in Fig. 7(b), shows variation between 0.47 and 0.18 ns (except at notches), thereby displaying appreciable linearity. The proposed filter covers a total circuit area of only 14.6×7.3 mm^2.

Conclusion

This paper presents a compact UWB filter with dual notches at 5.8 and 8 GHz. The hybrid microstrip/CPW transition technology is utilized to develop the basic UWB filter, wherein a short-circuited SIR is present within a CPW in the ground and is vertically coupled to two microstrip lines on the top. The optimized coupling of this alignment develops a four pole UWB-BPF with good insertion/return loss. The dual passband notches and extended stopband are implemented using the transmission zeros of SDGS (etched in SIR in the ground plane) and four SRRs (coupled to I/O lines) on top. The *S* parameters and group delay of the experimental prototype exhibits appreciable agreement with the simulated data. These pleasing frequency characteristics combined with its miniaturized size makes the proposed structure a necessary additive to any UWB communication system.

Acknowledgements. The authors appreciate Sunrays Circuits, Bangalore, for their generous help in filter's fabrication.

References

1. Revision of Part 15 of the Commission's Rules Regarding Ultra-Wideband Transmission Systems', First Note and Order Federal Communications Commission, ET-Docket, 2002, 98–153.
2. **Wu HW and Chen YF** (2012) New compact ultra wideband bandpass filter using modified multi- mode resonator. *International Journal of Electronics and Communications (AEÜ)* **66**, 1021–1025.
3. **Chu QX and Huang JQ** (2010) Compact ultra-wideband filter with dual notched bands based on complementary split ring resonators. *Microwave and Optical Technology Letters* **52**, 2509–2512.
4. **Liu BW, *et al.*** (2011) Compact UWB bandpass filter with two notched bands based on electromagnetic bandgap structures. *Electronics Letters* **47**, 757–758.
5. **Liu BW, *et al.*** (2012) Design of compact UWB bandpass filter with dual notched bands using novel SCRLH resonator. *Microwave and Optical Technology Letters* **54**, 1506–1508.
6. **Zhao J, *et al.*** (2013) Compact microstrip UWB bandpass filter with dual notched bands using E-shaped resonator. *IEEE Microwave and Wireless Components Letters* **23**, 638–640.
7. **Nouri S, *et al.*** (2017) Design and analysis of compact BPF with dual notch bands based on stepped-impedance resonator for UWB applications. *Microwave and Optical Technology Letters* **59**, 672–674.
8. **Wei F, *et al.*** (2013) Ultra-wideband band-pass filter with dual narrow notched bands based on dual-mode stepped impedance resonator. *Microwave and Optical Technology Letters* **55**, 727–730.
9. **Song K and Xue Q** (2010) Compact ultra-wideband (UWB) bandpass filters with multiple notched bands. *IEEE Microwave and Wireless Components Letters* **20**, 447–449.
10. **Mohammadi B, *et al.*** (2015) Design of a compact dual-band-notch ultra-wideband bandpass filter based on wave cancellation method. *IET Microwaves, Antennas & Propagation* **9**, 1–9.
11. **Ghazali A and Singh A** (2016) Band Notched UWB-BPF based on broadside coupled microstrip/CPW transition. *IETE Journal of Research* **62**, 686–693.
12. **Ghazali A and Singh A** (2014) Broadside coupled UWB filter with dual notched band and extended upper stopband. *International Conference on Devices, Circuits and Communications (ICDCCom)*, 1–5.
13. **Song Y, Yang GM and Geyi W** (2014) Compact UWB bandpass filter with dual notched bands using defected ground structures. *IEEE Microwave and Wireless Components Letters* **24**, 230–232.
14. **Ghazali A and Pal S** (2013) Planar ultra-wideband filter with triple notches and improved out-of-band performance. *IEEE MTT-S International Microwave and RF Conference*, 1–4.
15. **Ghazali A and Pal S** (2013) Microstrip based UWB filter with controllable multiple notches and extended upper stopband. *International Conference on Emerging Trends in Communications, Control, Signal Processing and Computing Applications (C2SPCA)*, 1–5.
16. **Baik JW, Lee TH and Kim YS** (2007) UWB bandpass filter using microstrip-to-CPW transition with broadband balun. *IEEE Microwave and Wireless Components Letters* **17**, 846–848.
17. **Gao J, *et al.*** (2005) Short-circuited CPW multiple-mode resonator for ultra-wideband (UWB) bandpass filter. *IEEE Microwave and Wireless Components Letters***16**, 104–106.
18. **Zhu L, Sun S and Menzel W** (2005) Ultra-wideband (UWB) bandpass filters using multiple-mode resonator. *IEEE Microwave and Wireless Components Letters* **15**, 796–798.
19. **Sun S and Zhu L** (2009) Multiple-mode-resonator-based bandpass filters for ultrawideband transmission systems. *IEEE Microwave Magazine* **10**, 88–98.

https://doi.org/10.1017/S1759078718000594 Published online by Cambridge University Press

Abu Nasar Ghazali received his B.Tech. degree in Electronics & Communication Engineering (ECE) from SRM University, Chennai, in 2008 and M.E. degree in Microwave Engineering from Birla Institute of Technology (BIT) Mesra, in 2010 where he was a GATE scholar. He completed his doctorate in 2014 from BIT Mesra. He worked as an Assistant Professor (I) in the Department of ECE at the BIT Mesra, Patna campus. Currently, he is an Assistant Professor (II) in the School of Electronics Engineering, at the Kalinga Institute of Industrial Technology (KiiT), Bhubaneswar, India. He is an Associate member, The Institution of Engineers (IEI), India and member of IEEE. He has published quite a few papers in SCI/SCOPUS indexed journals and conferences. His main research interests are UWB filters, Microstrip filters, and passive microwave circuit components.

Mohd Sazid received his B.Tech. degree in ECE from Uttar Pradesh Technical University in 2011 and M.E. degree in Wireless Communication Engineering from BIT Mesra in 2015 where he was a GATE scholar. He is currently working as an Assistant Professor in the Department of ECE at the Noida Institute of Engineering & Technology. He has published several papers in SCI indexed journals. His main research interests are UWB filters and microstrip-based passive circuit components.

Srikanta Pal received his B.Tech. degree in Electronics & Communication Engineering from NIT Warangal, India and M.Tech. degree in Microwave Engineering from Jadavpur University, Kolkata, India in 1990 and 1992, respectively. From 1992 to 2000 he was with the R&D Antenna Lab of the Bharat Electronics Limited (BEL). In 2001, he joined the Oxford University as a Research Associate where he worked toward his Ph.D. on HTS Microwave Filters, which he completed in 2003. From 2003 to 2005 he was a visiting Faculty in the Centre for Advanced Research in Electronics (CARE) Department at the IIT Delhi, India. In 2005, he joined the Department of Electronics and Computer Engineering at the IIT Roorkee, India, as an Assistant Professor. He joined the Emerging Devices Technology Center at the Birmingham University as a Post Doctorate fellow in 2006 where he designed a HTS filter which is currently installed in the world's largest Telescope, Green Bank Telescope (GBT), West Virginia, USA. In 2008, he joined the ECE Department at the BIT Mesra where he is currently working as a Professor and Head of the Department. He is also a lifetime Research Fellow at the University of Birmingham. His research interests include RF Filters and Devices, MEMS, HTS Microwave filters, Antennas and Computational Electromagnetics.

https://doi.org/10.1017/S1759078718000594 Published online by Cambridge University Press